Aggregation of Double-Tailed Ionic Liquid 1,3-Dioctylimidazolium Bromide and the Interaction with Triblock Copolymer F127

ARTICLE *in* THE JOURNAL OF PHYSICAL CHEMISTRY B · NOVEMBER 2013

Impact Factor: 3.3 · DOI: 10.1021/jp405838v · Source: PubMed

5 AUTHORS, INCLUDING:

ge Lingling
Yangzhou University
28 PUBLICATIONS **136** CITATIONS

SEE PROFILE

THE JOURNAL OF PHYSICAL CHEMISTRY B

Article

pubs.acs.org/JPCB

Aggregation of Double-Tailed Ionic Liquid 1,3-Dioctylimidazolium Bromide and the Interaction with Triblock Copolymer F127

Lingling Ge, Qi Wang, Duo Wei, Xiaohong Zhang, and Rong Guo*

School of Chemistry and Chemical Engineering, Yangzhou University, Jiangsu Province 225002 People's Republic of China

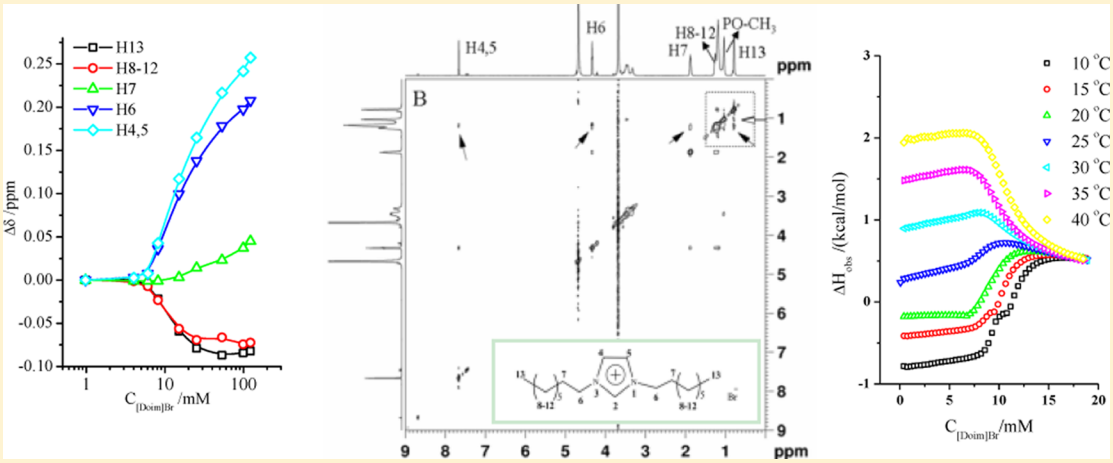

ABSTRACT: The aggregation of ionic liquid-based double-tailed surfactant, 1,3-dioctylimidazolium bromide ([Doim]Br) and its interaction with pluronic copolymer F127 were systematically investigated by nuclear magnetic resonance (NMR), surface tension, dynamic light scattering (DLS), and isothermal titration calorimetry (ITC). It was found that the [Doim]Br aggregates are composed with the alkyl chains embedded in the micellar core and with the imidazolium rings parallel and staggered on the hydrophilic layer of micelles, which was generally different from the single-tailed IL [omim]Br. The hydrogen bonding between protons attached to the imidazolium rings and anion Br^- was enhanced upon the aggregation of [Doim]Br. The aggregation of F127 was promoted by addition of [Doim]Br, which was more efficient than the single-tailed surfactant. At lower [Doim]Br content, [Doim]Br monomers embedded deeply into F127 micelle core. At higher [Doim]Br concentrations, the F127 micelles were disassociated, and then F127 chains penetrated into [Doim]Br micelle. In addition, the microstructure of F127/[Doim]Br complex can also be tuned by temperature.

INTRODUCTION

Ionic liquids (ILs) have entered into researchers' sight since the 1940s. They are classified as organic salts. The steric hindrance of the huge ion disfavors their formation of crystals and subsequently lowers the melting points. The resultant large liquid range and negligible vapor pressure, as well as their thermal stability and nonflammability make ILs green replacements for the traditional volatile organic solvents in chemical procedures.[1] Surface active ILs generate specific self-assembled structures in aqueous solution. The aggregates can act as a novel micellar catalyst and perform enhanced template action for the synthesis of nanostructured materials.[2] Hence, the investigation on the self-assembling of ILs is of great interest. Many reports[2−4,5a,6] elucidated the roles of different factors on the aggregation such as the type of cations, the nature of counterions, and the alkyl chain length. Headley et al.[7,10] have revealed the effect of counterions on the hydration of imidazolium based on NMR measurements. Wang et al.[9] applied the quantum chemical calculations to study the interaction between water and ILs with different counterions [Cl^-], [Br^-], [BF_4^-], and [PF_6^-]. All the results above showed that the cation, as well as ion pair, could interact with water. It was also reported that the ionic hydration, the cation−anion association, and the aggregation of ILs offset each other.[2c] In addition, the alkyl chain length plays an important role in the aggregation of ILs. It is found that long alkyl chains hinder the interaction between the rings and water, which is favorable to the aggregation.[2c,10] Gemini imidazolium surfactants processing two headgroups and two alkyl chains have lower critical micellization concentration (cmc), and show the tendency to form premicellar aggregation at sufficiently low concentration.[11]

Scientific research developed from the beginning with the basic physical properties, as well as their aggregation behaviors in the pure surface active IL systems,[2] to very recently the mixed systems of ILs with small molecules,[2a,3] synthetic polymers,[4] and biomacromolecules.[5] Investigations on the

Received: June 13, 2013
Revised: November 11, 2013
Published: November 14, 2013

interaction between surface active ILs and amphiphilic block copolymer, such as triblock copolymer poly(ethylene oxide)−poly(propylene oxide)−poly(ethylene oxide) (PEO−PPO−PEO), are of great interest. Because the block copolymer would affect the aggregation behavior of ILs by forming the IL/copolymer complex driven mainly by the hydrophobic force and the electrostatic interaction. As reported by Singh et al.,[3] poly(ethylene oxide) and its derives reduced the spontaneity of the aggregation of ILs. On the other hand, the presence of surface active ILs in the mixed systems of ILs/copolymer can also realize the control of the microstructure and subsequently the properties of copolymer solutions by friendly physical methods.[12,13] Studies in the mixed system of copolymer P123 and IL 1-pentyl-3-methylimidazolium tetrafluoroborate ([pmim][BF_4]) were performed by Adhikari et al.[4a] It has been found that the IL surfactant penetrated into the hydrophobic core of P123 micelles at lower concentrations and then invaded both the core and corona region, reducing the difference between the two regions. The presence of the ion pairs of ILs and their electrostatic repulsion may be responsible for the expansion of the polymer core. The same phenomena was observed in the system of copolymer P104 and 1-butyl-3-methyl-imidazolium bromide ([bmin]Br).[4b] In our group, the interaction mechanism and the binding mode of the copolymer with traditional nonionic surfactant Triton X-100[14] and functional nonionic surfactant, the hydrophilic modified anti-inflammatory drug ibuprofen,[15] have been systematically studied. The complexes with various microstructures were observed. More interestingly, the microstructures of these complexes were found to be turned by temperature and the concentration of surfactant.

In the present contribution, a new kind of double-tail surfactant, 1,3-dioctylimidazolium bromide ([Doim]Br), was synthesized, and the aggregation behavior of this novel ionic liquid-based surfactant was investigated. In addition, the interaction mechanism between [Doim]Br and F127 as well as the microstructure change of the complex was systematically studied.

EXPERIMENTS SECTION

Materials and Sample Preparation. Pluronic F127 of average composition $EO_{97}PO_{68}EO_{97}$ was obtained from Sigma Corp. and used without further purification; 2-dimethyl-2-silapentane-5-sulfonate sodium (DSS, >97%) was a Sigma product. Deuterium oxide (99.9%) was from Qing Dao Teng Long Corp., and 1-bromooctane (99%) was purchased from Shanghai Chemical Corp.

Ionic liquid [Doim]Br was synthesized by two steps. First, metal sodium (7.6 g) was added to the anhydrous ethanol (about 100 mL) gradually to form ethanol−sodium ethylate stock solution. Imidazole (20.0 g) was then put into the stock solution and subsequently 1-bromooctane (59.6 mL) was added when solid imidazole disappeared. The reaction solution was stirred at 65 °C for 20 h, and then a yellow liquid was obtained. The liquid was washed by water and extracted by anhydrous ethyl ether, which were repeated two times or more. The anhydrous ethyl ether was removed by rotary evaporator, and finally 1-octylimidazole was gained (>90%). Second, 1-octylimidazole (6.5 mL) and 1-bromooctane (6.9 mL) were mixed and stirred at 100 °C for 20 h with the protection of nitrogen. After the yellow viscous liquid was washed by light petroleum and the light petroleum was wiped off by a rotary evaporator, the product [Doim]Br was gained (Scheme 1).

Scheme 1. Molecular Structure of [Doim]Br

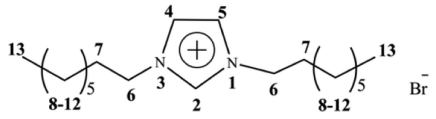

^{1}H NMR: 10.822 ppm (S, 1H, C2−H), 7.239 ppm (S, 2H, C4, C5−H), 4.368 ppm (T, 4H, C6−H), 1.927−1.275 ppm (M, 24H, C7−H), 0.874 ppm (T, 6H, C8−H). ^{13}C NMR: 137.085 ppm (C2), 122.132 ppm (C4,5), 50.145 ppm (C6, 2), 31.681 ppm (C7, 2), 30.360 ppm (C8, 2), 29.048 ppm (C9, 2), 28.968 ppm (C10, 2), 26.263 ppm (C11, 2), 22.582 ppm (C12, 2), 14.060 ppm (C13, 2). Element analysis (% in mass) calculated: C, 61.11; H, 9.99; N, 7.5. Found: C, 60.46; H, 9.79; N, 7.26. HPLC purity: 97.2%.

Surface Tension Measurement. Isothermal surface tension measurements were carried out by the DCAT 11 surface tension device (Data physics Instruments GmbH, German) using the platinum plate mode. The surface tension was determined with a single-measurement mode. The results were accurate within 0.1 mN/m. Before each measurement, distilled water was used as a calibration and the value was 72.0 ± 0.1 mN/m. The temperature was controlled by water bath, and the uncertainty was within ±0.1 °C.

Nuclear Magnetic Resonance (^{1}H NMR). The NMR experiments were conducted on a Bruker Avance 600 spectrometer with a ^{1}H frequency of 600.13 MHz. The temperature was kept constant within ±0.1 °C by a Bruker BCU-05 temperature control unit. The samples were allowed to equilibrate at the desired temperature for at least 10 min before measurement. A total of 32 accumulations was generally acquired. A stock solution of 0.003 M DSS in D_2O in a capillary was inserted into the sample tube as a reference, which was used to eliminate the temperature-induced shifts. D_2O was used as solvent. The temperature ranged from 5 to 40 °C, and the interval was 5 °C. The data at [Doim]Br concentration higher than 50 mM could not be obtained at a temperature lower than 15 °C, due to the limitation of solubility in D_2O. The error of chemical shifts value obtained was within ±0.01 ppm.

Two-dimensional hydrogen nuclear Overhauser effect spectroscopy (2D NOESY) experiments were performed at 30 °C with a standard three-pulse sequence.[16] A mixing time of 600 ms and 32 scans for each of the 1024 t_1 increments were recorded.

Dynamic Light Scatter (DLS). The DLS experiments have been described in detail in ref 17. In this study, all solutions were filtered through a Millipore filter with 0.22 μm pore size. In addition, all the samples were heated from lower to higher temperature to eliminate the difference caused by heating and cooling during the temperature effect study.[18] The temperature was controlled by pumping the water bath to the sample holder, and the uncertainty of the temperature was ±0.1 °C. The samples were thermostated at the desired temperature for at least 10 min before measurements. Measurements were carried out at a scattering angle of 90°. Experiment duration was 5 min, and each experiment was repeated two times or more.

Isothermal Titration Calorimetry (ITC). The calorimetry experiments were performed using a titration microcalorimeter (Microcal VP-ITC, North Hampton, MA) at temperatures of 10 ± 0.1 and 30 ± 0.1 °C.[14] A computer-controlled syringe (250 μL) was filled with the [Doim]Br solution at higher

dx.doi.org/10.1021/jp405838v | J. Phys. Chem. B 2013, 117, 15014−15022

concentrations, which was titrated into a 1.438 mL sample cell containing purified water or 20 mg/mL F127 aqueous solution. The volume of each injection was 5 μL, and the time delay between successive injections was 360 s. The stirring speed was maintained at 502 rpm to ensure thorough mixing.

Conductivity Measurement. The conductivities of the [Doim]Br solutions were carried out using a DDS-11A digital conductivity meter (Shanghai Tianda Precision Instrument Co. Ltd.) calibrated by KCl aqueous solution.

RESULTS AND DISCUSSION

Surface Tension Measurement. Figure 1 shows the surface tension curve of 1,3-dioctylimidazolium bromide

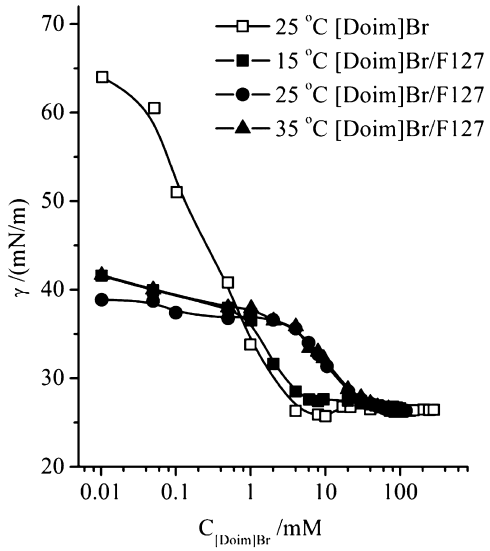

Figure 1. Surface tension in the system [Doim]Br/F127/H_2O at various temperatures. The concentration of F127 is 20 mg/mL. The surface tension of [Doim]Br aqueous solution at 25 °C is also presented. The temperature uncertainty is within ±0.1 °C.

([Doim]Br) in the absence and presence of F127. The surface tension in the absence of F127 starts to decrease from about 64.0 mN/m to about 25.9 mN/m at a [Doim]Br concentration of 8.0 mM, where the surface tension remains constant. The concentration of 8.0 mM at the break point is ascribed to the critical micellar concentration (cmc) of [Doim]Br. The surface tension of single chain surfactant 1-methyl-3-octylimidazolium bromide ([omim]Br) has been measured by Wang et al.[2e] The cmc of [omim]Br is about 120 mM, which is about 15 times higher than that of [Doim]Br, and the plateau surface tension value is as high as 35.0 mN/m. These results indicate that [Doim]Br, which has the double symmetrical aliphatic chains, has remarkably higher surface activity. As for the curves in the presence of F127, the initial surface tension value at the lowest concentration of [Doim]Br investigated is only about 38 mN/m, which is close to the value in the system F127/H_2O, indicating that the air/water surface is occupied mostly by F127 chains. The surface tension decreases with further addition of [Doim]Br due to the adsorption of [Doim]Br molecules onto the surface. The final plateau surface tension values are the same as that in pure [Doim]Br solutions, which indicates that most of the F127 chains on the surface are replaced by [Doim]Br molecules that are of higher surface activity. It should be noted that the cmc value of [Doim]Br in the presence of F127 gets much higher, indicating that the interaction of [Doim]Br with F127 suppresses the self-aggregation of [Doim]Br. As reported in ref 18, the aggregation behavior of the copolymer strongly depends on temperature, mainly because the hydration state of the PPO blocks is temperature sensitive. The hydrophobicity of the PPO blocks will increase upon heating due to the disrupted hydrogen bond between ether oxygen and water. The reported critical micellization temperature (cmt) for 20 mg/mL F127 aqueous solution is about 25 °C.[14] In the present study, the surface tension curve shifts to higher [Doim]Br concentration as the temperature rises from 15 to 25 °C. This shift of surface tension curves and the increased cmc value of [Doim]Br indicate that the interaction between [Doim]Br and F127 is enhanced with rising temperature, from which we can deduce that the hydrophobic interaction between PPO blocks and the alkyl chains of [Doim]Br is probably one of the main driving forces. At temperatures higher than the cmt, no further difference of surface tension is observed, which suggests that the temperature-enhanced interaction is saturated.

NMR Measurement. Figure 2 shows the plot of the chemical shift variation $\Delta\delta$ of [Doim]Br protons. Inter alia, $\Delta\delta$

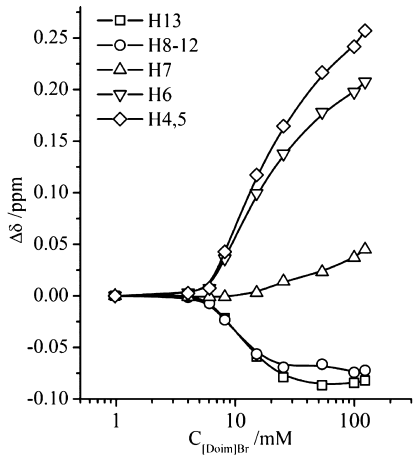

Figure 2. [Doim]Br concentration dependence of $\Delta\delta$ for [Doim]Br protons at 25 ± 0.1 °C. $\Delta\delta = \delta_{obs} - \delta_{ori}$, where δ_{ori} is the chemical shift value at the lowest [Doim]Br concentration under study.

$= \delta_{obs} - \delta_{ori}$, where δ_{ori} is the chemical shift value at the lowest [Doim]Br concentration under study and δ_{obs} is the observed chemical shift at higher [Doim]Br concentrations. No signal for H2 is observed due to the deuteration. It is worthy to mention that the protons at the same position on the two symmetrical alkyl chains have the same chemical shift value, which further indicates that the chemical environment of the two alkyl chains is uniform. From Figure 2 we can find that all the $\Delta\delta$ values keep constant at lower [Doim]Br concentrations. Obvious changes of $\Delta\delta$ are observed at [Doim]Br concentrations higher than 8.0 mM, which is defined as the cmc of [Doim]Br. The cmc value agrees with that determined by surface tension measurement. An abrupt increase of protons H4,5 on the imidazolium ring as well as nearby protons H6, is observed, whereas $\Delta\delta$ values of protons H8−12 and H13 on the alkyl chains decrease. In addition, no obvious variation of $\Delta\delta$ for the proton H7 is observed.

The double-tailed ILs exist as monomers in diluted solutions, and both the cations and anions are highly dissociated and hydrated. As the monomers transfer from water to aggregates above the cmc, the double tails are immersed into the hydrophobic micellar core, and the hydrophilic imidozalium

dx.doi.org/10.1021/jp405838v | J. Phys. Chem. B 2013, 117, 15014−15022

rings stay on the surface of the micelle and remain hydrated. Along with the cations, anion Br^- will also be transferred from water to the micellar surface, resulting in increased local concentration and hence the enhanced cation−anion association.[2c,8,19] The conductivity profile of the [Doim]Br solution is shown in Figure 3. Two linear regions are obtained. and the

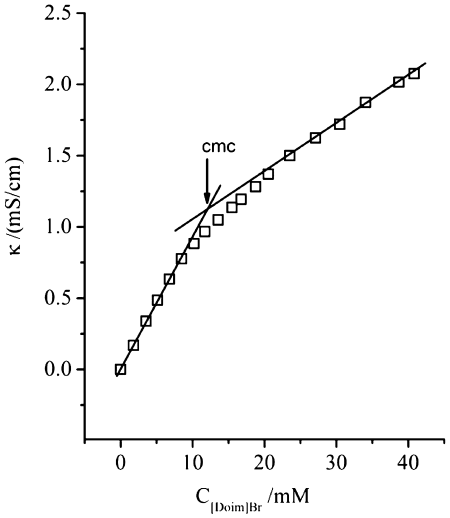

Figure 3. Electric conductivity (κ) of [Doim]Br solution as a function of concentration at 25 ± 0.1 °C. The cmc values are denoted by vertical marks.

break of the conductivity curve originates from the micellization of [Doim]Br. The cmc value is in good agreement with the values determined by surface tension and NMR measurements.[20] The slope of the linear region above the cmc is smaller than that below the cmc, indicating an effective loss of ionic charges owing to the binding of counterions on the micellar surface. This phenomenon verifies the enhanced cation−anion association. As reported by Singh et al.,[3] the protons on the imidazolium ring, e.g., H2 and H4,5 including proton H6 on the side chains, are acidic due to the vicinity of electronegative nitrogen. They tend to form hydrogen bonding with the anion Br^- and water. The enhanced hydrogen bonding between the protons H4,5,6 and Br^- leads to a downfield shift.[21] What is more, the protons lying outside the shielding cone of the imidazolium ring experience a downfield shift, because the imidazolium ring is conventionally aromatic and capable of sustaining a ring current.[2c,21,22] It has been confirmed that the imidazolium rings arrange in a stack way with the rings parallel and staggered.[2c,21,22] Thus, the proton H4,5 and H6 lying outside the shielding cone would undergo a downfield shift upon the micellization as the ion pairs get closer. The enhanced hydrogen bonding as well as the ring current is verified by the increased chemical shift of proton H4,5, as well as H6 (Figure 2). It should be noted that the extent of increase in chemical shift upon the micellization of double-tailed [Doim]Br is much higher than that of single-tailed [omim]Br.[2c] This phenomenon is attributed to more significantly enhanced hydrogen bonding upon micellization, because the initial contact between [Doim]Br monomers and solvent is much weaker due to the steric hindrance of two long hydrophobic side chains.[10] As for the alkyl protons H8−13, the dehydration and subsequently interrupted deshielding effect should be the main reason for the upfield shift upon aggregation. In addition, a partial structural change of the alkyl chain from trans to gauche conformation will also occur upon aggregation and contribute to the upfield shift of alkyl protons.[2a] The chemical shift change of proton H7 in the vicinity of polar head groups is not obvious, as they locate at the interface between the hydrophilic layer and hydrophobic core where the effects mentioned above offset each other.[3]

For the mixed system F127/[Doim]Br/H_2O, the effect of [Doim]Br on the temperature-induced aggregation of F127 is investigated by the chemical shift change of PO−CH_3 protons (Figure 4).[14,23] The chemical shift curve of pure F127 aqueous

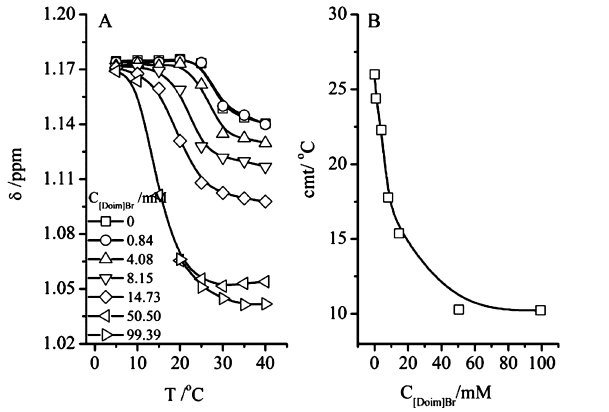

Figure 4. (A) Temperature-dependent ^1H NMR chemical shifts of PO−CH_3 protons in 20 mg/mL F1 27 aqueous solution at different [Doim]Br concentrations. (B) [Doim]Br concentration dependence of the cmt of F127. The temperature uncertainty is ±0.1 °C.

solution agrees with the result reported.[14] The initially higher constant δ value at 1.17 ppm indicates highly hydrated PO blocks due to the deshielding effect from the hydrogen bond between ether oxygen and water, and the polymers exist as water-swollen random coils.[23] An abrupt decrease of δ value corresponds to the temperature-induced breakdown of the hydrogen bond and subsequently the aggregation of the PO block to form the hydrophobic core of the copolymer micelle. The first inflection of the chemical shift curve is ascribed to the critical micellization temperature (cmt) and the value obtained for 20.0 mg/mL F127 aqueous solution is about 26 °C, which agrees well with the value reported.[14] Upon addition of [Doim]Br, the initial δ value remains at about 1.17 ppm, suggesting the unchanged hydration degree of the F127 random coil. What is more, all the δ curves exhibit the same manner at all the concentrations of [Doim]Br investigated. Similar phenomena are observed in the mixed system F127/TX-100, but only within the lower surfactant concentration region (<9.42 mM).[14] Within the higher TX-100 concentration region (27.85−95.85 mM), the increased initial δ values at lower temperatures as well as the reincrease of the δ value at higher temperatures are reported. The increased initial δ value is ascribed to the stretching effect on F127 unimers induced by the adsorption of TX-100 micelles. The reincrease of the δ value is caused by the microstructural rearrangement of the F127/TX-100 complex. In the present system F127/[Doim]Br, neither of these two phenomena is observed. The main reason is the smaller size of [Doim]Br aggregates, which will be further demonstrated in the Dynamic Light Scatter section. In addition, the final constant δ value of each curve keeps decreasing with increasing [Doim]Br content, from about 1.14 ppm to about 1.03 ppm, whereas the lowest δ value in the system F127/TX-100 is as high as about 1.12 ppm. The decrease in δ value

dx.doi.org/10.1021/jp405838v | J. Phys. Chem. B 2013, 117, 15014−15022

mainly originates from the improved hydrophobic interaction between PPO blocks and [Doim]Br. The lower δ values imply that the double-tailed surfactant is more efficient than the single-tailed surfactant in complexation with F127. The cmt values in the mixed systems of F127/[Doim]Br can be obtained from the curves in Figure 4A. The value keeps decreasing with increasing amount of [Doim]Br till 50.50 mM (Figure 4B), after which the value tends to be constant, indicating that the interaction between F127 and [Doim]Br is saturated. The reduced cmt value indicates that the addition of [Doim]Br promotes the aggregation of F127.

The microenvironment the change of [Doim]Br protons upon complexation with F127 is also monitored. As shown in Figure 5A (hollow symbols), the lower the chemical shift of the terminal alkyl proton H13, the higher the concentration, which indicates that proton H13 transfers from the bulk to the hydrophobic micellar core. In addition, the δ values of H13 keep decreasing with rising temperature at all [Doim]Br concentrations investigated, which originates from the disturbance of the water structure around the alkyl chains of [Doim]Br by heating. In the mixed system F127/[Doim]Br/D_2O, an "S" shape is observed at lower concentrations of [Doim]Br. The temperature at the first intersection of the δ curve happens to be the same as the cmt values of F127 in the mixed system. This phenomenon indicates that [Doim]Br molecules are solubilized into F127 micelles driven by the hydrophobic force. Proton H13 then experiences a more hydrophilic environment because the hydrophobicity of the PPO core is lower than that of the premicellar core of [Doim]Br.[24] At higher concentrations of [Doim]Br, the δ values of H13 in the mixed system exhibit a linear increase with rising temperature. It is probably because the PPO chains of F127 gradually penetrate into [Doim]Br micelles due to improved hydrophobic properties of the PPO chain.[24] It should be noted that the data at 5 and 10 °C are missed at higher [Doim]Br concentrations, because the system becomes turbid in D_2O unlike in H_2O. Similar phenomena have been reported,[25] and the reason is the different structure of D_2O and H_2O. Compared with the cases of the alkyl protons, two main differences are observed in the δ value of imidazolium ring protons H4,5 (Figure 5B). The first is that the higher the chemical shift, the higher the concentration of [Doim]Br. The reasons are the enhanced cation−anion association, the improved binding with water, and also the ring stacking in the micelles as discussed above. Second, the δ value of proton H4,5 shows a decrease with increased temperature, which is caused by the prominent dehydration of the imidazolium ring upon heating.

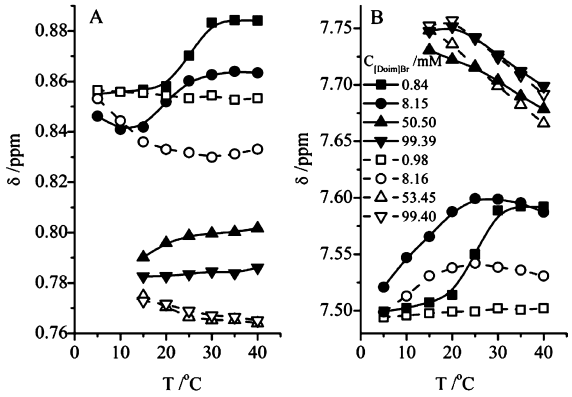

Figure 5. Temperature-dependent ^{1}H NMR chemical shifts of H13 (A) and H4,5 (B) signals of [Doim]Br aqueous solution in the absence (hollow symbols) and presence (filled symbols) of 20 mg/mL F127 at different [Doim]Br concentrations. The temperature uncertainty is ±0.1 °C.

Nuclear Overhauser effect spectroscopy (NOESY) is usually applied to provide information on the arrangement of molecules in space with the distance of the protons within 0.5 nm. The contour plots of the 2D NOESY spectra for the [Doim]Br/F127/D_2O system are shown in Figure 6. The concentrations of [Doim]Br are chosen to be lower and higher than cmc, and the F127 concentration is fixed. As shown in Figure 6, the cross peaks of H(8−12) with the nearby protons H7 and H13 are observed in both systems, and they mainly originate from intramolecular NOE.[26] By comparison, in the spectra at different concentrations of [Doim]Br (Figure 6A,B), the cross-peak between protons H(8−12) and H6 appears at a concentration higher than the cmc, which reflects their decreasing distance and subsequently verifies the aggregation of [Doim]Br monomers. Former investigations on the system of the single-tailed IL [omim]Br by Zhao et al.[2c] showed that alkyl chains of [omim]Br extended to the other two imidazolium rings verified by the cross peak between protons of the terminal methyl and the rings. In the present manuscript,

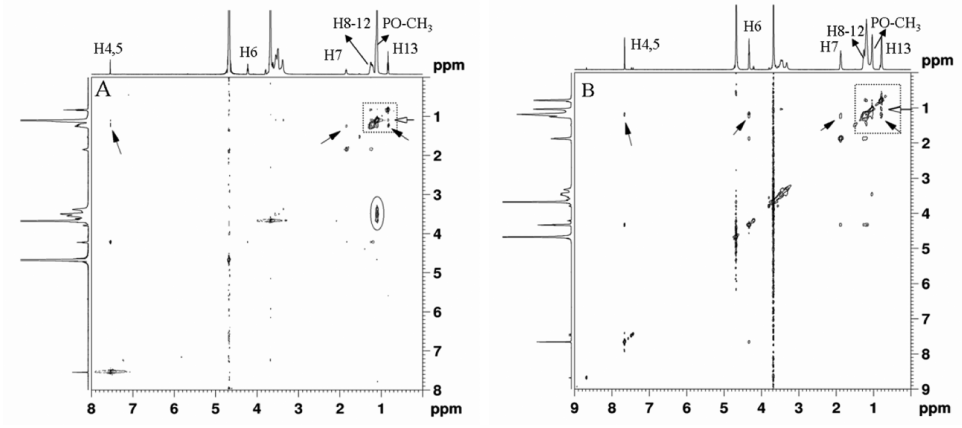

Figure 6. 2D NOESY spectra in the system [Doim]Br/F127/D_2O with [Doim]Br concentrations of 4.38 mM (A) and 60.22 mM (B) at 30 ± 0.1 °C. The concentration of F127 is fixed at 20 mg/mL.

dx.doi.org/10.1021/jp405838v | J. Phys. Chem. B 2013, 117, 15014−15022

no cross peak between protons H13 and H4,5 is observed, suggesting that the alkyl chains of [Doim]Br mainly embed in the core of [Doim]Br micelles apart from the imidazolium rings. F127 mainly exists as micelles at 30 °C.[15a] Thus, the disappearance of the cross peaks between EO−CH_2 protons and PO−CH_3 protons at higher [Doim]Br concentrations (the ellipse line, Figure 6) suggests the decomposition of F127 micelles. In addition, the cross peak of H13 and PO−CH_3 protons is observed at both [Doim]Br concentrations investigated, demonstrating their shorter distance regardless of the aggregation state of F127 and [Doim]Br. As a conclusion, [Doim]Br monomers embed deeply into the F127 micelle core at lower [Doim]Br content. The F127 micelles are disassociated at higher concentrations accompanied by F127 chains penetrating into [Doim]Br micelles.

DLS Measurement. Figure 7A shows the relaxation time distribution ($\tau A(\tau)$) versus $\log(\tau/\mathrm{ms})$ in the system [Doim]Br/H_2O at various [Doim]Br concentrations. A slow mode at around 1.3 ms is observed at lower [Doim]Br concentrations (<cmc) with a hydrodynamic radius (R_h) of about 100 nm. This slow mode diminishes gradually with increasing concentration of [Doim]Br, and a faster mode appears at around 0.01 ms with a R_h of about 1.5 nm, which corresponds to the [Doim]Br micelle. Referring to the synthesis process of [Doim]Br, the larger aggregates probably come from the hydrophobic impurity. Higher integral area of the resonance peaks corresponding to the alkyl protons in the NMR spectrum also verifies this impurity (data were not shown). As the micelles are formed, the impurity is gradually solubilized into the hydrophobic core of the micelles, leading to the disappearance of the slow mode, which is similar to the case in F127 aqueous solution reported.[14] Figure 7B shows the temperature effect on the size of [Doim]Br micelles. The relaxation time distribution moves to faster time with increasing temperature, and the corresponding R_h value decreases from 2.58 to 0.75 nm. Two contrary effects on the micellization of surfactant are caused by the increase of temperature. They are the decrease in the hydration degree of the hydrophilic headgroups favorable to the micellization, and the disruption of the water structures surrounding the hydrophobic chains weakening the hydrophobic effect and subsequently unfavorable to the micellization.[2d] Due to highly solvated imidazolium ring at the surface of the micelle, the significant shrink might be mainly contributed by the dehydration of the rings, which is also verified by a faster decrease in the chemical shift of proton H4,5 compared to H13 (Figure 5).

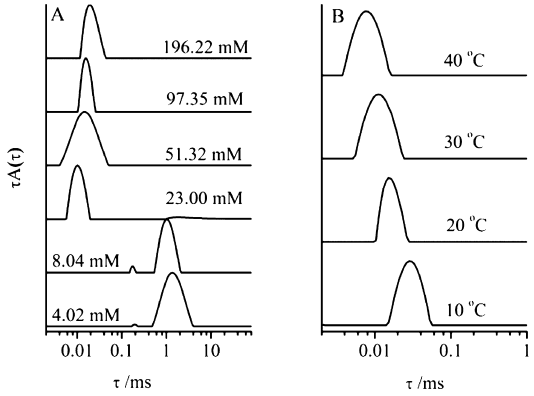

Figure 7. Variation of the relaxation time distributions for pure [Doim]Br aqueous solutions with varied concentrations at 20 °C (A) and varied temperatures at a [Doim]Br concentration of 97.35 mM (B). The temperature uncertainty is within ±0.1 °C.

Figure 8 shows the temperature induced change of relaxation time distribution in the mixed system F127/[Doim]Br/H_2O.

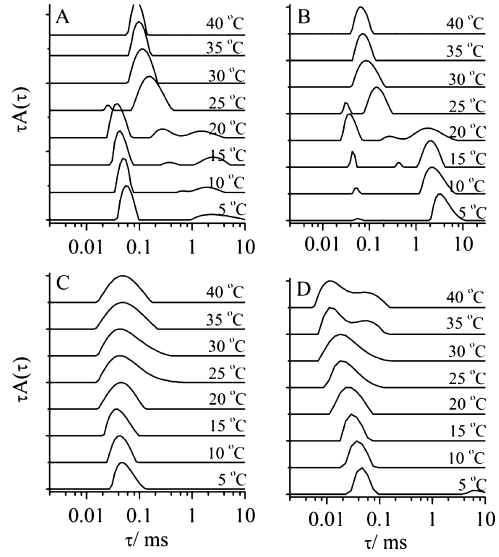

Figure 8. Relaxation time distributions at various temperatures for 20 mg/mL F127 aqueous solutions with increasing [Doim]Br concentrations (mM): (A)[17] no [Doim]Br; (B) 1.00; (C) 23.58; (D) 100.23. The temperature uncertainty is within ±0.1 °C.

At lower concentrations of [Doim]Br (Figure 8B), the relaxation distribution is bimodal at 5 °C. The faster mode corresponds to the F127 unimers. The slow mode is attributed to the clusters consisting of the hydrophobic components in the system.[27] Different from the case of the F127/H_2O system (Figure 8A),[14] the slow mode dominates the distribution curve because of the extra hydrophobic components from [Doim]Br as described above. The slow mode dramatically diminishes as the temperature rises to 20 °C accompanied by the appearance of a middle mode corresponding to the complex F127/[Doim]Br. The middle mode shifts to faster time and becomes prominent, accompanying the disappearance of both slow and fast modes. The formed F127/[Doim]Br complex solubilizes the extra hydrophobic components, leading to a dramatic decrease of the slow mode. The R_h value of the complex decreases from about 12.5 nm at 20 °C to about 5.9 nm at 40 °C. All the R_h values are smaller than the corresponding ones in F127 aqueous solutions.[14] This phenomenon might be attributed to the electro elastic repulsion between the imidazolium rings at the surface of the complexes, which inhibits the growth of the complex.[28] At a higher concentration of [Doim]Br (Figure 8C), a single mode is observed within all the temperature range investigated and turns out to be broad and unsymmetric at higher temperatures. The reported micellar cluster with F127 chains wrapping around several micelles as described in the F127/TX-100 system is not observed in the present system. The hydration radius R_h of the micelle of nonionic surfactant TX-100 is reported to be about 4.5 nm at 25 °C.[14] For IL-based surfactant [Doim]Br, the R_h value is around 1.5 nm, which is about one-third that of the TX-100 micelle. Thus, the stretching effect of [Doim]Br micelles on PPO chains and subsequently the formation of a micellar cluster are not as significant as that in the TX-100/F127

dx.doi.org/10.1021/jp405838v | J. Phys. Chem. B 2013, 117, 15014−15022

system. This conclusion is also verified by the unchanged chemical shift of proton PO−CH_3 (Figure 4A). The coexistence of [Doim]Br micelles and F127/[Doim]Br complex leads to one broad relaxation time distribution. At a [Doim]Br concentration of 100.33 mM, the amount of free [Doim]Br micelles increases. Thus, the distribution of free [Doim]Br micelles at higher temperatures becomes separate from that of the F127/[Doim]Br complex (Figure 8D).

ITC Measurement. The isothermal titration calorimetry (ITC) is a vital method to determine the cmc and the micellization enthalpy (ΔH_{mic}).[25,29] The values of micellization enthalpy (ΔH_{mic}) are determined from the enthalpy difference between the two linear segments of the enthalpy curves, as illustrated in Figure 9.[29,30] The observed enthalpy curves are

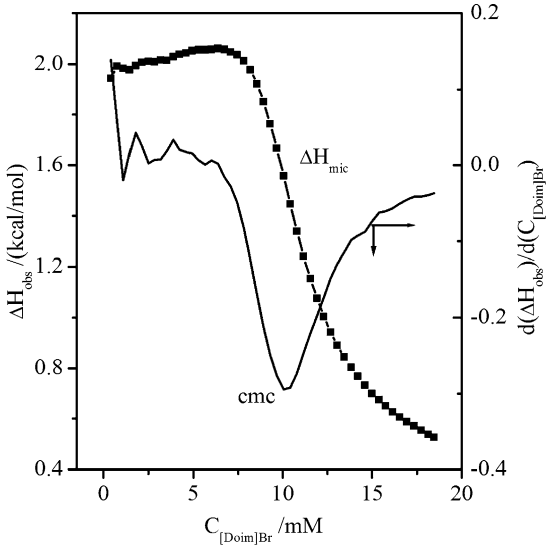

Figure 9. ITC curve of concentrated [Doim]Br solution titrated into water at 40 ± 0.1 °C and the first derivative of the curve calculated from the interpolated values.

fitted and then differentiated with respect to the concentration of [Doim]Br. The position of the extremum at differential curve is taken as the cmc.

The calorimetric titration curves of ΔH_{obs} at different temperatures are presented in Figure 10. The dilution curves

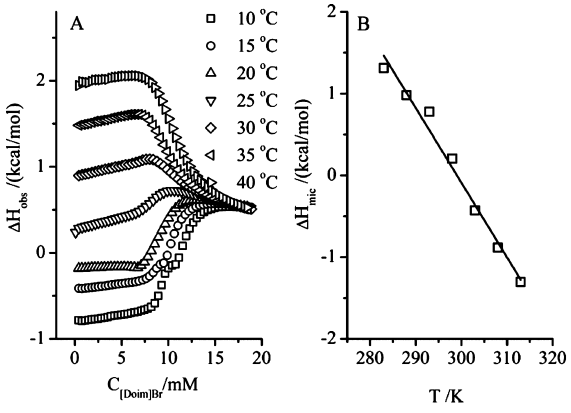

Figure 10. ITC curve of concentrated [Doim]Br solutions titrated into water at different temperatures (A) and the temperature dependence of the micellization enthalpy (B). The temperature uncertainty is within ±0.1 °C.

are sigmoidal in shape and are subdivided into two concentration regions separated by a transition region associated with micelle formation. The micellization process is exothermic at temperatures below 25 °C and then it becomes endothermic at higher temperatures. This phenomenon is similar to the case in the system nonylglucoside/H_2O,[31] which stems from the temperature dependence of the dilution enthalpies of concentrated micelles. The dependence of the derived ΔH_{mic} values on temperature is presented in Figure 10B. A linear decrease of ΔH_{mic} on temperature is observed. The difference in heat capacities of surfactants, $\Delta C_{p,mic}$, is obtained from the slope. The negative value of $\Delta C_{p,mic}$ reflects the hydrophobic segments of surfactant transferring from the bulk to micelles.[32] According to Jolicoeur and Gill et al.,[33] the absolute value of $\Delta C_{p,mic}$ is approximatively proportional to the fraction of the hydrophobic chains transferred. The fraction is represented by the number of hydrogen atoms (n_H) including those on the terminal methyl group and the intermediate methylene group.The equation $\Delta C_{p,mic} = -7.88 n_H$ cal/(mol·K) was therefore approximately built.[29a,30,34] The value n_H for double-tailed [Doim]Br is about 9 with the $\Delta C_{p,mic}$ value equal to −0.09 kcal/(mol·K) obtained from Figure 10B. It means that only about two methylene groups on each octyl chain of [Doim]Br are embedded into the micellar core besides one terminal methyl, and the rest of the alkyl chains remain hydrated. This deduction is confirmed by the remarkable temperature-induced shrink of [Doim]Br micelles due to dehydration determined by DLS (Figure 7B). The highly hydrated state of the alkyl chain in the micelle might originate from high steric hindrance of the double chains attaching on position 1,3 of the imidazolium ring.

The enthalpy profile for the titration of concentrated [Doim]Br solutions into aqueous solutions of F127, and pure water at 10 and 30 °C are shown in Figure 11. At 10 °C (Figure 11A),

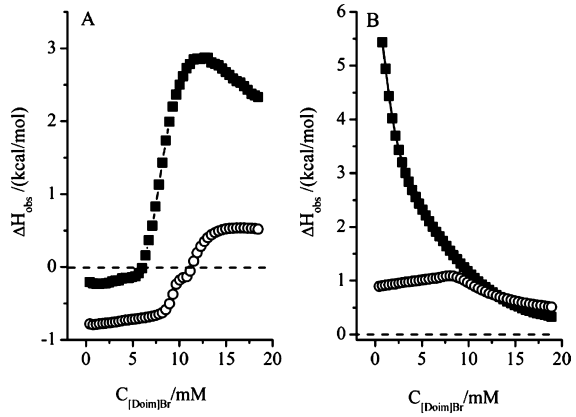

Figure 11. ITC curve of concentrated [Doim]Br solutions titrated into F127 aqueous solutions of 20 mM at 10 ± 0.1 °C (A) and 30 ± 0.1 °C (B). The results of concentrated [Doim]Br solutions titrated into water are shown for comparison (hollow symbols).

the ΔH_{obs} values in the mixed system start from higher values and exhibit a more significant increase with rising [Doim]Br concentration compared to that in [Doim]Br aqueous solutions. The endothermic effect is caused by the interaction between [Doim]Br and F127 unimers, which compensates the exothermic effect originating from the dilution of [Doim]Br micelles. The more significant increase in the mixed system is contributed by the dehydration of copolymer unimers, the

dx.doi.org/10.1021/jp405838v | J. Phys. Chem. B 2013, 117, 15014−15022

conformational changes of copolymer, and the interaction between surfactant and copolymer unimers. At 30 °C (Figure 11B), the ΔH_{obs} value for the first injection increases as high as 5.43 kcal/mol compared to 0.9 kcal/mol of pure [Doim]Br solutions. F127 unimers have completed the micellization at 30 °C, and hence, the high endothermic value is attributed to the interaction between F127 micelles and [Doim]Br. It is reported that the interactions between the copolymer and anion surfactant lead to the formation of the complex as polymer micelle/surfactant and further to a disruption of copolymer micelles.[35] The disruption of the F127 micelle would arise, which is an exothermic effect, resulting in a decrease of ΔH_{obs} with the concentration of [Doim]Br. At higher [Doim]Br concentrations, the formation of the complex with a skeleton of [Doim]Br micelles might lead to a slight rehydration of F127 chains, which leads to an exothermic effect showing a lower ΔH_{obs} value than in the system [Doim]Br/water.

■ CONCLUSIONS

The aggregation of double-tailed IL-based surfactant [Doim]Br and its interaction mechanism with F127 were investigated. The microstructure of [Doim]Br aggregates with the alkyl chains embedded in the micellar core and with the imidazolium rings parallel and staggered at micellar surface was proposed. The formation of [Doim]Br micelles was driven mainly by the hydrophobic interaction, as well as the enhanced hydrogen bonding between the imidazolium ring and anions. The steric hindrance of the double tail yields the higher hydrated micelles, which exhibits more significant temperature dependence on both the hydration state and the size.

The interaction model between [Doim]Br and F127 can be turned by temperature and the concentration of [Doim]Br. At lower temperatures, the stretching effect on the F127 chains exerted by the adsorption of [Doim]Br micelles is not as significant as that in the system of traditional surfactant TX-100 because of the smaller micelle size. At higher temperatures, the addition of [Doim]Br promotes the aggregation of F127 to form the [Doim]Br/F127 complex, which is more efficient than the single-tailed surfactant. With an increase of [Doim]Br concentration, the skeleton of the complex progressively changes from F127 micelles to [Doim]Br micelles.

■ AUTHOR INFORMATION

Corresponding Author

*R. Guo: e-mail, guorong@yzu.edu.cn; fax, (+86)-514-87311374.

Notes

The authors declare no competing financial interest.

■ ACKNOWLEDGMENTS

This work was financially supported by the National Nature Science Foundation of China (No. 21203162, 21073156), Project Funded by the Priority Academic Program Development of Jiangsu Higher Education Institutions, and Natural Science Fund for Colleges and Universities in Jiangsu Province (No. 13KJ13050040).

■ REFERENCES

(1) (a) Lee, J. K.; Kim, M. J. *J. Org. Chem.* **2002**, *67* (19), 6845−6847. (b) Welton, T. *Chem. Rev.* **1999**, *99* (8), 2071−2084. (c) Fischer, T.; Sethi, A.; Welton, T.; Woolf, J. *Tetrahedron Lett.* **1999**, *40* (4), 793−796. (d) Anderson, J. L.; Armstrong, D. W.; Wei, G. T. *Anal. Chem.* **2006**, *78* (9), 2892−2902. (e) Wasserscheid, P.; Keim, W. *Angew. Chem., Int. Ed.* **2000**, *39* (21), 3772−3789. (f) Hussey, C. L.; Barnard, P. A.; Sun, I. W.; Appleby, D.; Hitchcock, P. B.; Seddon, K. R.; Welton, T.; Zora, J. A. *J. Electrochem. Soc.* **1991**, *138* (9), 2590−2594.

(2) (a) Singh, T.; Kumar, A. *J. Phys. Chem. B* **2007**, *111* (27), 7843−7851. (b) Shi, L.; Zheng, L. *J. Phys. Chem. B* **2012**, *116* (7), 2162−2172. (c) Zhao, Y.; Gao, S.; Wang, J.; Tang, J. *J. Phys. Chem. B* **2008**, *112* (7), 2031−2039. (d) Dong, B.; Zhao, X.; Zheng, L.; Zhang, J.; Li, N.; Inoue, T. *Colloids Surf. A* **2008**, *317* (1−3), 666−672. (e) Wang, J.; Wang, H.; Zhang, S.; Zhang, H.; Zhao, Y. *J. Phys. Chem. B* **2007**, *111* (22), 6181−6188.

(3) Singh, T.; Rao, K. S.; Kumar, A. *J. Phys. Chem. B* **2012**, *116* (5), 1612−1622.

(4) (a) Adhikari, A.; Dey, S.; Das, D. K.; Mandal, U.; Ghosh, S.; Bhattacharyya, K. *J. Phys. Chem. B* **2008**, *112* (20), 6350−6357. (b) Zheng, L.; Guo, C.; Wang, J.; Liang, X.; Chen, S.; Ma, J.; Yang, B.; Jiang, Y.; Liu, H. *J. Phys. Chem. B* **2007**, *111* (6), 1327−1333.

(5) (a) Ding, Y.; Zhang, L.; Xie, J.; Guo, R. *J. Phys. Chem. B* **2010**, *114* (5), 2033−2043. (b) Zhou, T.; Xu, G. Y.; Ao, M. Q.; Yang, Y. L.; Wang, C. *Colloids Surf. A* **2012**, *414*, 33−40.

(6) (a) Reddy, P. M.; Venkatesu, P. *J. Phys. Chem. B* **2011**, *115* (16), 4752−4757. (b) Wang, L.; Wu, Z.; Pei, M.; Wu, X.; Tao, X. *Chin. J. Chem.* **2010**, *28* (7), 1069−1075.

(7) Headley, A. D.; Jackson, N. M. *J. Phys. Org. Chem.* **2002**, *15* (1), 52−55.

(8) Lin, S. T.; Ding, M. F.; Chang, C. W.; Lue, S. S. *Tetrahedron* **2004**, *60* (42), 9441−9446.

(9) Wang, Y.; Li, H.; Han, S. *J. Phys. Chem. B* **2006**, *110* (48), 24646−24651.

(10) Headley, A. D.; Kotti, S. R. S. S.; Nam, J.; Li, K. *J. Phys. Org. Chem.* **2005**, *18* (10), 1018−1022.

(11) (a) Kamboj, R.; Singh, S.; Bhadani, A.; Kataria, H.; Kaur, G. *Langmuir* **2012**, *28* (33), 11969−11978. (b) Pal, A.; Datta, S.; Aswal, V. K.; Bhattacharya, S. *J. Phys. Chem. B* **2012**, *116* (44), 13239−13247.

(12) Sardar, N.; Kamil, M.; Kabir ud, D. *Ind. Eng. Chem. Res.* **2011**, *51* (3), 1227−1235.

(13) Li, X.; Wettig, S. D.; Verrall, R. E. *Langmuir* **2004**, *20* (3), 579−586.

(14) Ge, L.; Guo, R.; Zhang, X. *J. Phys. Chem. B* **2008**, *112* (46), 14566−77.

(15) (a) Wei, D.; Ge, L.; Guo, R. *Colloid Polym. Sci.* **2013**, 1−11. (b) Wei, D.; Ge, L.; Ding, Y.; Guo, R. *Colloids Surf. A* **2013**, *421* (0), 16−25.

(16) Ernst, R. R.; Bodenhausen, G.; Wokaun, A., *Principles of nuclear magnetic resonance in one and two dimensions*; Oxford University Press: New York, 1987.

(17) Ge, L.; Zhang, X.; Guo, R. *Polymer* **2007**, *48* (9), 2681−2691.

(18) Ma, J.; Guo, C.; Tang, Y.; Liu, H. *Langmuir* **2007**, *23* (19), 9596−9605.

(19) Shimizu, S.; Pires, P. A. R.; Fish, H.; Halstead, T. K.; El Seoud, O. A. *Phys. Chem. Chem. Phys.* **2003**, *5* (16), 3489−3497.

(20) Dong, B.; Gao, Y.; Su, Y.; Zheng, L.; Xu, J.; Inoue, T. *J. Phys. Chem. B* **2010**, *114* (1), 340−348.

(21) Avent, A. G.; Chaloner, P. A.; Day, M. P.; Seddon, K. R.; Welton, T. *J. Chem. Soc., Dalton Trans.* **1994**, *0* (23), 3405−3413.

(22) Bonhôte, P.; Dias, A. P.; Papageorgiou, N.; Kalyanasundaram, K.; Grätzel, M. *Inorg. Chem.* **1996**, *35* (5), 1168−1178.

(23) Ma, J.; Guo, C.; Tang, Y.; Wang, J.; Zheng, L.; Liang, X.; Chen, S.; Liu, H. *Langmuir* **2007**, *23* (6), 3075−3083.

(24) Wanka, G.; Hoffmann, H.; Ulbricht, W. *Macromolecules* **1994**, *27* (15), 4145−4159.

(25) Kresheck, G. C. *J. Phys. Chem. B* **1998**, *102* (34), 6596−6600.

(26) Cui, X. H.; Jiang, Y.; Yang, C. S.; Lu, X. Y.; Chen, H.; Mao, S. Z.; Liu, M. L.; Yuan, H. Z.; Luo, P. Y.; Du, Y. R. *J. Phys. Chem. B* **2010**, *114* (23), 7808−7816.

(27) Löf, D.; Schillén, K.; Loh, W.; Olofsson, G. *J. Phys. Chem. B* **2007**, *111* (21), 5911−5920.

(28) Nambam, J. S.; Philip, J. *J. Phys. Chem. B* **2012**, *116* (5), 1499−1507.

(29) (a) Jiang, N.; Li, P.; Wang, Y.; Wang, J.; Yan, H.; Thomas, R. K. *J. Phys. Chem. B* **2004**, *108* (39), 15385−15391. (b) Li, Y.; Reeve, J.; Wang, Y.; Thomas, R. K.; Wang, J.; Yan, H. *J. Phys. Chem. B* **2005**, *109* (33), 16070−16074.
(30) Bai, G.; Wang, J.; Yan, H.; Li, Z.; Thomas, R. K. *J. Phys. Chem. B* **2001**, *105* (39), 9576−9580.
(31) (a) Majhi, P. R.; Blume, A. *Langmuir* **2001**, *17* (13), 3844−3851. (b) Stodghill, S. P.; Smith, A. E.; O'Haver, J. H. *Langmuir* **2004**, *20* (26), 11387−11392. (c) Prasad, M.; Chakraborty, I.; Rakshit, A. K.; Moulik, S. P. *J. Phys. Chem. B* **2006**, *110* (20), 9815−9821.
(32) (a) Shinoda, K. *J. Phys. Chem.* **1977**, *81* (13), 1300−1302. (b) Rodríguez, J. R.; González-Pérez, A.; Del Castillo, J. L.; Czapkiewicz, J. *J. Colloid Interface Sci.* **2002**, *250* (2), 438−443.
(33) (a) Jolicoeur, C.; Philip, P. R. *Can. J. Chem.* **1974**, *52* (10), 1834−1839. (b) Gill, S. J.; Wadsö, I. *Proc. Natl. Acad. Sci. U. S. A.* **1976**, *73* (9), 2955−2958.
(34) Li, Y.; Li, P.; Wang, J.; Wang, Y.; Yan, H.; Thomas, R. K. *Langmuir* **2005**, *21* (15), 6703−6706.
(35) Barbosa, S.; Taboada, P.; Castro, E.; Mosquera, V. *J. Colloid Interface Sci.* **2006**, *296* (2), 677−684.